Macromolecules 1981, *14*, 1463–1468

Trans Placements, Expansion, and Asymmetry of Starlike Polyethylenes Bearing Similarly Charged Ends

Wayne L. Mattice* and Jeffrey Skolnick

Department of Chemistry, Louisiana State University, Baton Rouge, Louisiana 70803.
Received March 24, 1981

ABSTRACT: Average configuration-dependent physical properties have been evaluated for tri-, tetra-, and hexafunctional polymethylene stars perturbed by electrostatic repulsion of charges placed at the free chain ends. Configuration-dependent properties evaluated were the probability for a trans placement, expansion of $\langle s^2 \rangle$, the mean-square radius of gyration, asymmetry of the distribution of chain atoms, and asymmetry of the distribution described by the atoms considered to bear the charges. Perturbations disappear as n, the number of bonds, becomes infinite. When n is a few hundred, the perturbation no longer affects the probability of a trans placement, but it still produces significant alterations in both $\langle s^2 \rangle$ and asymmetry. The characteristic ratio, $\langle s^2 \rangle / nl^2$, for all three types of stars goes through a maximum as n increases in a medium of low dielectric constant. However, the manner in which the increase in $\langle s^2 \rangle$ is accommodated along the three principal axes depends on both n and the functionality of the branch point.

Linear bolaform electrolytes, i.e., molecules with the chemical structure $Y^-X^+(CH_2)_xX^+Y^-$, are simple molecules which possess some of the characteristics of polyelectrolytes.[1] Thus electrostatic interaction causes primary and secondary dissociation constants for bolaforms of finite x to differ by more than the ratio (4) expected in the absence of any interaction of the chain ends. The ratio of dissociation constants must become 4 as x becomes infinite. Configuration-dependent properties of the intervening polymethylene chain can be altered by electrostatic interaction of charged chain ends in the completely dissociated bolaform, $X^+(CH_2)_xX^+$. For example, if x is about 10^2, interaction of charged chain ends produces an enhanced probability that a bond will occupy a trans placement, an increase in mean-square radius of gyration, and an increased asymmetry of the distribution of chain atoms.[2] While these changes are all in the direction which brings about an approach to rodlike behavior, such bolaforms are nevertheless more accurately described as coils than as rods.[2] There is another regime, $\infty > x \gg 10^2$, where there is no significant affect on the probability of a trans placement, but the chain is nonetheless expanded and has a higher asymmetry than that seen in the unperturbed state.[2] Chain expansion, in the absence of any alteration in the probability of a trans placement, can also be observed with chains perturbed through attachment of an end to an impenetrable interface[3] and in chains expanded by the intramolecular excluded volume effect.[4,5]

Our concern here is with branched-molecule equivalents of linear bolaform electrolytes. A general formula for the completely dissociated form of these molecules is $Z[(CH_2)_xX^+]_f$, where Z denotes the branch point of the f-functional star. These stars are perhaps primitive schematic models for micelles formed by aggregation of f molecules of the form $H(CH_2)_xX^+$. Linear bolaform electrolytes are obtained with $Z = CH_2$, $f = 2$. Three branched bolaforms are treated here: (a) $f = 3$, Z = CH; (b) $f = 4$, Z = C; (c) $f = 6$, Z = carbon skeleton of benzene. The only perturbation considered is that arising from electrostatic interaction of charged chain ends. Configuration-dependent properties of interest are the molecular expansion, alteration in the probability for observation of a trans placement, distortion of the asymmetry of the distribution of all chain atoms, and asymmetry of the distribution described by atoms at the charged chain ends.

Calculations

Bond Angles, Bond Lengths, and Rotational States. That portion of the molecule sufficiently remote from the branch point was treated using a rotational isomeric state model which successfully rationalizes configuration-dependent properties of unperturbed polymethylene.[6,7] The C–C bond length and CCC angle are held constant at 153 pm and 112°, respectively. Internal bonds have three rotational states with dihedral angles of 0° (t) and ±120° ($g^{\pm}$). First- and second-order interactions are accommodated using $\sigma = 0.54$ and $\sigma = 0.088$. Here σ is the weight of $g^{\pm}$ relative to t, and $\sigma^2\omega$ is the weight of $g^{\pm}g^{\mp}$ relative to tt.

Branch point geometry differs from that used for linear polymethylene. The angle CC′C is 111° if C′ constitutes a trifunctional branch point.[8] A tetrafunctional branch point has tetrahedral geometry. First- and second-order interactions in tri- and tetrafunctional stars are accommodated using branched-molecule rotational isomeric state formalism.[9] Detailed composition of the statistical weight matrices used for bonds near the branch point is that described earlier.[10,11] Parameter assignment was $\sigma = \tau = 0.54$, $\omega = 0.088$, $\psi = 1$.

The carbon skeleton of benzene is constructed by using a bond length of 140 pm and a bond angle of 120°. Each $C–C^{ar}–C^{ar}$ angle is also 120°, and the $C–C–C^{ar}$ angle is 112° (C^{ar} denotes a carbon atom in the benzene ring). The $C–C–C^{ar}–C^{ar}$ dihedral angles were maintained at ±90°, with the sign assigned so that neighboring branches depart in opposite directions from the planar aromatic unit. Rotational states, and statistical weights, for the remaining bonds in each branch were those appropriate for an unperturbed linear polymethylene chain. Thus the only influence of one branch on another in the hexafunctional star is in the requirement that neighboring branches depart the planar aromatic unit in opposite directions.

Representative Samples of Chains. Representative samples of chains were generated by using a priori and conditional probabilities computed from the configuration partition function in the manner detailed in ref 9. This procedure properly takes account of all first- and second-order interactions at the branch point in tri- and tetrafunctional stars. Each molecule is assigned an energy $\sum_{i=1}^{f-1}\sum_{j=i+1}^{f} e^2/Dr_{ij}$, where e denotes the electronic charge, D the dielectric constant, and r_{ij} the separation of atoms at the free ends of chains i and j. Molecules are weighted according to $\exp(-\text{energy}/kT)$, with T being 140 °C. Calculations were performed with 3.5, 10, 30, 100, and ∞ for the dielectric constant. The unperturbed state is obtained with $D = \infty$, and $D = 3.5$ is a reasonable approximation to the macroscopic dielectric constant in many organic solvents. As in our earlier study of linear bolaforms,[2] neither counterions nor a supporting electrolyte is taken into consideration in the weighting scheme. If

0024-9297/81/2214-1463$01.25/0

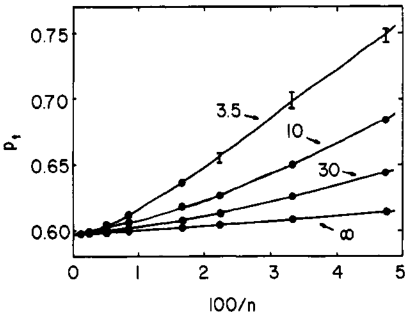

Figure 1. Probability for observation of a trans placement in a trifunctional bolaform containing n bonds when the medium has the indicated dielectric constant.

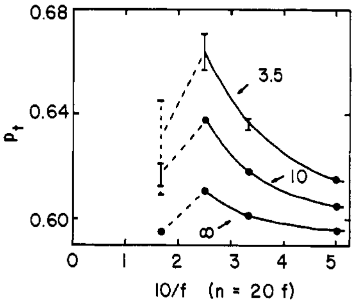

Figure 2. Probability for observation of a trans placement in f-functional bolaforms having 20 bonds in each branch, the medium having the indicated dielectric constant.

counterions or a supporting electrolyte were present, they would cause all weighting factors to lie closer to unity, thereby diminishing the perturbation produced by interaction of charged chain ends.

The total number of bonds in the f-functional star is denoted by n. Each branch contains n/f bonds. In most cases, 50×10^3 molecules were generated at each n and divided into five sets of 10×10^3 stars each. Configuration-dependent properties for each star were calculated in the same manner used for linear bolaforms.[2] They were averaged for the weighted molecules in each group. The radius of plotted points is as large as, or larger than, the standard deviation of averages for the five sets containing 10×10^3 stars each. In those cases where the standard deviation is larger than the radius of plotted points, an error bar denoting ±1 standard deviation is used. For certain of the larger stars, computations were practical only if the number of molecules generated was less than 50×10^3.

Results and Discussion

Probability of a Trans Placement. Figure 1 depicts the probability, p_t, of a trans placement at bonds in the trifunctional stars. Only $n - 6$ bonds are considered in evaluation of p_t because the rotational state is not well-defined for bonds to atoms at the branch point or free chain ends. In the unperturbed linear polymethylene chain, p_t approaches 0.596 as n becomes infinite.[12] Results depicted in Figure 1 demonstrate that the same asymptotic limit is obtained with trifunctional stars. At small n, however, p_t exceeds 0.596 even when the stars are unperturbed ($D = \infty$). The increase in p_t at small n in unperturbed stars is a consequence of the great opportunity for repulsive short-range interactions between atoms in different branches when there are gauche placements at bonds near the branch point. This problem does not arise in the unperturbed linear polymethylene chain, causing its p_t to be more nearly independent of n in the range covered by Figure 1.[2]

The dependence of p_t on n becomes more pronounced when the perturbation produced by repulsive interaction of the charged chain ends is strong. This perturbation causes an increase in the probability of a trans placement. A qualitatively similar effect was observed with linear bolaforms immersed in media of finite dielectric constant.[2] However, the perturbation becomes larger upon going from linear to trifunctional bolaforms. For example, when n is 21 and D is 3.5, the linear bolaform has a p_t of about 0.64,[2] but Figure 1 shows p_t has the much larger value of 0.75 when the bolaform is trifunctional. A larger perturbation is seen in the trifunctional bolaform because there are three, rather than two, charged ends, and only 2/3 as many bonds intervene between each pair of charges.

A second consequence of the perturbation produced by repulsive interaction of charged chain ends is to increase the uncertainty in configuration-dependent physical properties evaluated for molecules in the representative sample of stars. When n is 30, for example, the uncertainty in p_t is small enough to merit plotting in Figure 1 as a filled circle if D is 10 or greater. If D is 3.5, however, the standard deviation becomes substantially larger than the radius of the filled circles used in preparation of this figure. Thus an error bar, of size ±1 standard deviation, is used for $n = 30$, $D = 3.5$. The increase in uncertainty arises in spite of the fact that precisely the same 50×10^3 stars (five sets of 10×10^3 stars each) were used for all D at $n = 30$. When D is infinite, each of the stars generated is given the same weight. However, as D becomes small, certain of the stars are given a much larger weight than others. In the limit of very small D, the average of a configuration-dependent property for the 10×10^3 weighted stars in a set may be dominated by a few molecules with relatively large weights. The average for another set of 10×10^3 weighted stars may be dominated by a few stars with somewhat different properties. Consequently, the standard deviation rises because the *effective* sample size declines as D decreases.

Figure 2 depicts behavior of p_t for f-functional bolaforms having 20 bonds in each branch. Results for the linear bolaform ($f = 2$) are from ref 2. In the unperturbed state, p_t increases as f rises from 2 to 4. The origin of this behavior lies in repulsive short-range interactions between atoms in different branches when bonds near the branch point occupy gauche states, as described above. These interactions are properly assessed in the statistical weight matrices used for bonds near the tri- and tetrafunctional branch points.[9-11] That such is the case is emphatically demonstrated by the behavior of the hexafunctional bolaform. In this case (see Calculations) the only influence of one branch on another is in the absolute requirement that neighboring branches depart in opposite directions from the planar aromatic unit. Otherwise the branches are assumed to behave as linear polymethylene chains, causing essentially identical p_t at $f = 2$ and 6 when the dielectric constant is infinite.

Without exception, repulsive interaction of charged chain ends produces an increase in p_t for the f-functional bolaforms for which results are depicted in Figure 2. If this effect is superimposed on that arising from repulsive short-range interactions near the branch point in the unperturbed state, p_t rises rapidly as $1/f$ decreases (see Figure 2 for f = 2–4). However, if no additional repulsive interactions are considered near the branch point, the rise in p_t with a decrease in $1/f$ is much less striking (see Figure 2 for $f = 2$ and 6). These limited results suggest that repulsive electrostatic interactions alone could not produce a p_t of unity, even at large f, when there are 20 bonds in

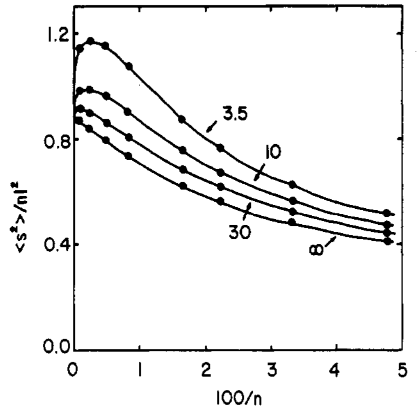

Figure 3. Characteristic ratios for trifunctional bolaforms containing n bonds when the medium has the indicated dielectric constant.

each branch. Electrostatic interaction of the charged chain ends cannot overcome the tremendous entropy reduction accompanying complete suppression of configurations having one or more gauche placements. This result in turn suggests electrostatic interactions alone could not produce a p_t of unity in a micelle formed by aggregation of f molecules of $H(CH_2)_{20}X^+$.

Mean-Square Radius of Gyration. Figure 3 depicts characteristic ratios for trifunctional stars. The characteristic ratio is defined as $\langle s^2 \rangle / nl^2$, where $\langle s^2 \rangle$ denotes the mean-square radius of gyration and l denotes the bond length. Characteristic ratios for unperturbed trifunctional stars undergo a monotonic increase as n increases.[10,13-15] The asymptotic limit is 7/9 of the limiting value for the unperturbed linear polymethylene chain,[16] as expected.[10,13-15,17,18] Qualitatively similar behavior is obtained with the tetra- and hexafunctional stars (not shown), asymptotic limits in these cases being 5/8 and 4/9, respectively, of the limit for the unperturbed linear polymethylene chain, as expected.[10,13-15,17,18]

The perturbation produced by electrostatic repulsion of charged chain ends must vanish as n becomes infinite. Therefore curves at all D have a common asymptotic limit. At intermediate n, however, repulsion of charged chain ends produces significant expansion when the medium has a low dielectric constant. This expansion can be so large that it causes the characteristic ratio to pass through a maximum at finite n. Comparison of Figures 1 and 3 demonstrates that significant expansion of trifunctional stars persists even when n becomes large enough so that p_t is indistinguishable from its unperturbed value. The same observation has been made for linear bolaforms[2] and for tetra- and hexafunctional bolaforms (not shown). Chain expansion tends to be larger in stars than in linear bolaforms. When D is 3.5, for example, the maximum values for α are 1.16, 1.21, 1.35 ± 0.02, and 1.34 ± 0.04 for $f = 2$, 3, 4, and 6, respectively. Here α^2 is defined as the ratio of $\langle s^2 \rangle$ at $D = 3.5$ to $\langle s^2 \rangle$ at $D = \infty$. Maximum expansion is obtained when n is between 100 and 600.

Figure 4 depicts expansion factors for stars having 20 bonds in each branch. The smallest expansion is seen with the linear bolaform ($f = 2$). At $D = 3.5$, a larger expansion is seen with the tetrafunctional star than with the hexafunctional star. This behavior arises in part because tetrafunctional stars experience maximal expansion when there are about 35 bonds in each branch, but maximal expansion for a hexafunctional star is not attained until each branch has about 80 bonds.

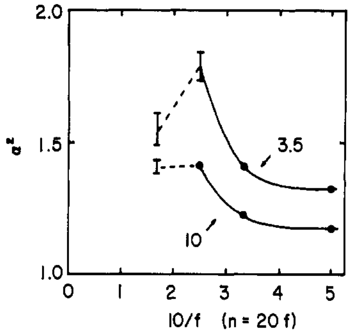

Figure 4. Expansion factors for f-functional bolaforms having 20 bonds in each branch. The definition of α^2 is the ratio of $\langle s^2 \rangle$ when D is 3.5 (or 10) to $\langle s^2 \rangle$ when D is infinite.

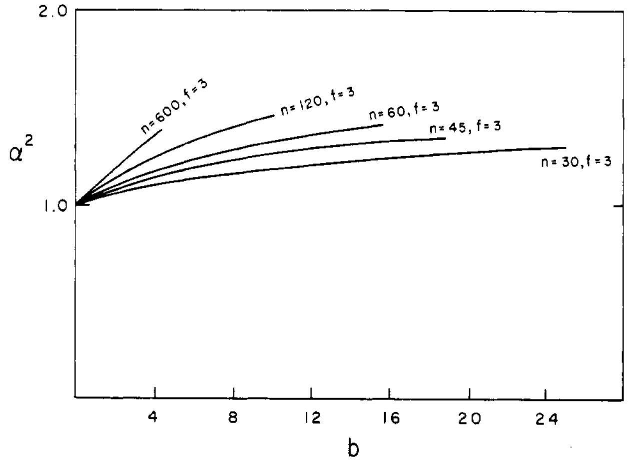

Figure 5. Expansion factor, α^2, as a function of b for trifunctional bolaforms.

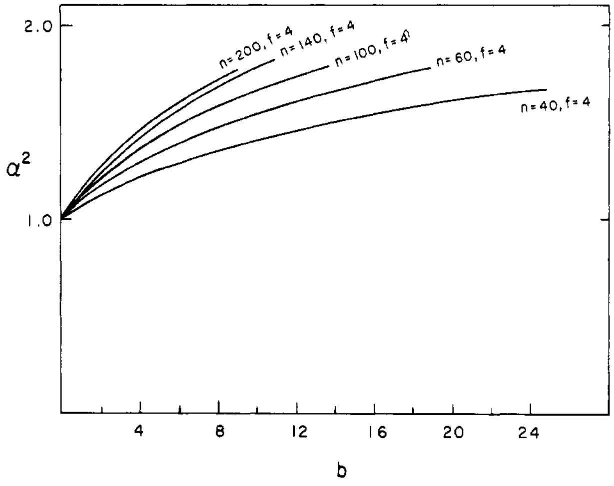

Figure 6. Expansion factor, α^2, as a function of b for tetrafunctional bolaforms.

Figures 5 and 6 depict α^2 as a function of $b = (e^2/DkT)(3/2\langle s^2 \rangle_0)^{1/2}$ for $f = 3$ and $f = 4$, respectively. Here b is the ratio of the characteristic length of electrostatic interactions, $l_e = e^2/DkT$, to an average dimension of a molecule in the absence of electrostatic repulsions. Increasing l_e relative to $\langle s^2 \rangle_0^{1/2}$ should produce a greater expansion of the molecule, as is indeed observed. Similar to the case of linear bolaforms, for a particular value of n all values of α^2 lie on the same curve, and the family of curves seems to converge to an upper limit as n becomes infinite.[2] Comparison of Figures 5 and 6 reveals larger expansion factors at a given b when $f = 4$ relative to that for $f = 3$. This observation is easily rationalized. An f-branched molecule contains f repelling ends. With a given kind of branch point geometry, if $f_1 > f_2$, $\alpha_{f1}^2 > \alpha_{f2}^2$.

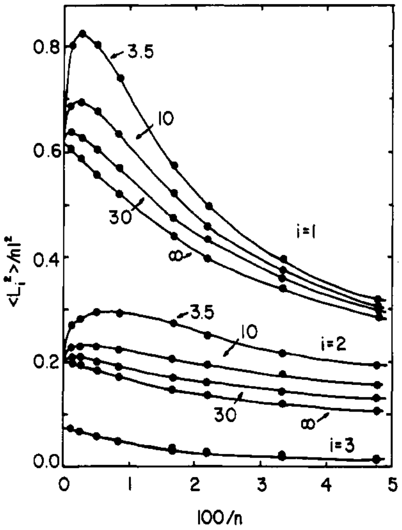

Figure 7. Averages of corresponding principal moments for the distribution of all chain atoms in trifunctional bolaforms containing n bonds, the medium having the indicated dielectric constant. Changes in $\langle L_3^2\rangle/nl^2$ due to repulsive interaction of the chain ends are not detectable on the scale used to prepare this figure.

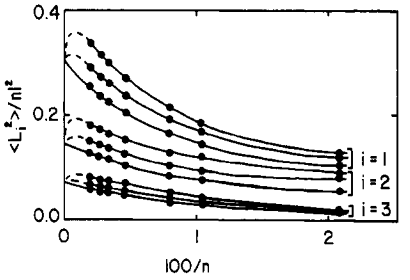

Figure 8. Averages of corresponding principal moments for the distribution of all chain atoms in hexafunctional bolaforms containing n bonds. For each i, the largest $\langle L_i^2\rangle$ is obtained with $D = 10$, the smallest with $D = \infty$, and the intermediate $\langle L_i^2\rangle$ with $D = 30$.

Table I
Limiting $\langle L_i^2\rangle/nl^2$ for Unperturbed f-Functional Polyethylene Stars

f	$(\langle L_1^2\rangle/nl^2)_\infty$	$(\langle L_2^2\rangle/nl^2)_\infty$	$(\langle L_3^2\rangle/nl^2)_\infty$
2	0.880	0.198	0.072
3	0.620	0.202	0.072
4	0.466	0.182	0.071
6	0.299	0.143	0.070

Similar observations hold for hexafunctional bolaforms.

Asymmetry of the Distribution of Chain Atoms. Asymmetry of the distribution of chain atoms is assessed by first finding the principal moments, L_i^2, for each individual configuration. Principal moments are indexed so that $L_1^2 \geq L_2^2 \geq L_3^2$, and, of course, $s^2 = L_1^2 + L_2^2 + L_3^2$. Averages of corresponding principal moments for all representative stars are denoted by $\langle L_i^2\rangle$. Their behavior for trifunctional stars is depicted in Figure 7. In the unperturbed state, each $\langle L_i^2\rangle/nl^2$ experiences a monotonic increase as n increases. Asymptotic limits at infinite n are in accord with $\langle L_2^2\rangle/\langle L_1^2\rangle = 0.326$ and $\langle L_3^2\rangle/\langle L_1^2\rangle = 0.116$, as must be the case for any trifunctional star.[13,19]

Electrostatic interaction of charged chain ends has no effect on $\langle L_i^2\rangle/nl^2$ when n is infinite. At finite n, however, repulsion of charged chain ends can produce a significant increase in $\langle L_1^2\rangle$ and $\langle L_2^2\rangle$. Changes also occur in $\langle L_3^2\rangle$, but they are not large enough to be apparent on the scale used in preparation of Figure 7. When n is less than about 60 (20 or fewer bonds per branch), expansion of the trifunctional star occurs preferentially in $\langle L_2^2\rangle$. When immersed in a medium of low dielectric constant, chain atoms in the small trifunctional stars are nearly all found to be lying in a plane defined by the larger two principal axes. Furthermore, if D and n are sufficiently small, the distribution along the second principal axis is nearly as large as that along the major principal axis. The distribution of chain atoms is approaching that represented by an ellipse whose axial ratio differs little from unity. Maximum separation of the three charged chain ends would be achieved if the three branches were coplanar and if the angle between each pair of branches was 120°. That configuration would have $\langle L_1^2\rangle = \langle L_2^2\rangle$, and $\langle L_3^2\rangle$ would be nearly zero. Clearly small trifunctional stars are driven toward, but do not actually attain, this configuration.

A different manner of expansion is found in trifunctional stars when n is a few hundred. Expansion then occurs preferentially along the major principal axis.

Figure 8 depicts averaged principal moments for hexafunctional stars. Once again each unperturbed $\langle L_i^2\rangle/nl^2$ is seen to experience a monotonic increase as n rises. Asymptotic limits are collected in Table I for the f-functional stars. The decrease in radius of gyration accompanying an increase in branch point functionality is seen to occur preferentially in the largest principal moment. Indeed, the smallest principal moment is nearly independent of functionality when f is 2–6. These same asymptotic limits apply to stars in which the only perturbation arises from electrostatic repulsion of the charged chain ends.

At finite n certain consequences of the expansion are common to tri-, tetra-, and hexafunctional stars. As shown by Figures 7 and 8, the expansion at small n occurs preferentially in $\langle L_2^2\rangle$, but at larger n it is $\langle L_1^2\rangle$ which experiences the largest change. The major qualitative change in the nature of the expansion when f rises from 3 to 6 is in its consequence for $\langle L_3^2\rangle$. The smallest principal moment is barely affected with trifunctional stars (Figure 7) but experiences significant expansion when the stars are hexafunctional (Figure 8). Averaged principal moments for $D = 3.5$ are not presented in Figure 8 because the family of curves for $\langle L_2^2\rangle$ would then overlap that for $\langle L_1^2\rangle$. No such overlap was seen with trifunctional stars (Figure 7). Overlap arises with hexafunctional stars, not because $\langle L_2^2\rangle$ has become more sensitive to the perturbation but rather because the *unperturbed* $\langle L_1^2\rangle$ has been markedly reduced, bringing it closer to the unperturbed $\langle L_2^2\rangle$ (Table I).

Figure 9 depicts ratios of averaged principal moments for f-functional bolaforms in which each branch contains 20 bonds. Electrostatic interaction of charged chain ends in the linear bolaform ($f = 2$) depresses both $\langle L_2^2\rangle/\langle L_1^2\rangle$ and $\langle L_3^2\rangle/\langle L_1^2\rangle$.[2] Expansion causes this bolaform to approach a rodlike distribution, although true rodlike behavior ($\langle L_1^2\rangle = \langle s^2\rangle$, $\langle L_2^2\rangle = \langle L_3^2\rangle = 0$) cannot be attained with a dielectric constant of physically meaningful size.[2] Expansion of trifunctional bolaforms also brings about a decline in $\langle L_3^2\rangle/\langle L_1^2\rangle$, but there is now an increase in $\langle L_2^2\rangle/\langle L_1^2\rangle$ because of the large change in $\langle L_2^2\rangle$ (Figure 7). Both $\langle L_2^2\rangle/\langle L_1^2\rangle$ and $\langle L_3^2\rangle/\langle L_1^2\rangle$ increase when bolaforms of functionality greater than 3 are expanded by repulsive interaction of their charged chain ends. These bolaforms are rendered less asymmetric by the perturbation. However, spherical asymmetry ($\langle L_1^2\rangle = \langle L_2^2\rangle = \langle L_3^2\rangle$) cannot be attained if the dielectric constant is assigned a physically meaningful value.

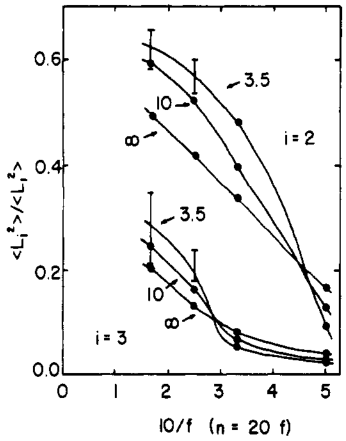

Figure 9. Ratios of averages of corresponding principal moments for the distribution of all chain atoms in *f*-functional bolaforms having 20 bonds in each branch, the medium being assigned the indicated dielectric constant.

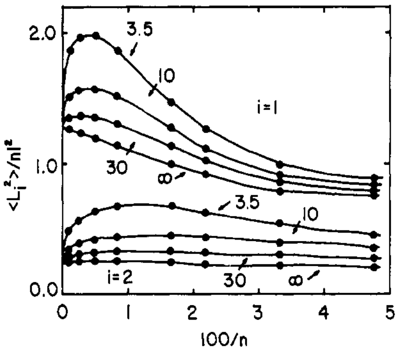

Figure 10. Averages of corresponding principal moments for the distribution of atoms at the chain ends in trifunctional bolaforms containing *n* bonds, the medium having the indicated dielectric constant.

Asymmetry of the Distribution of Charged Atoms. The preceding section was concerned with asymmetry of the distribution of chain atoms. Attention is now directed to asymmetry of the distribution of atoms at chain ends, i.e., those atoms considered to bear the charges. Since the trifunctional bolaform has only three charges, and three points describe a plane, each configuration has $s^2 = L_1^2 + L_2^2$ if the only points considered are the atoms at the chain ends. Figure 10 depicts the behavior of $\langle L_1^2 \rangle$ and $\langle L_2^2 \rangle$. Trends seen are similar to those observed when all chain atoms contributed to $\langle L_i^2 \rangle$ (Figure 7). Thus both $\langle L_i^2 \rangle$ undergo a monotonic increase with increasing *n* in the unperturbed state. The perturbation produces an increase in both $\langle L_i^2 \rangle$ at finite *n*, with the increase being concentrated in $\langle L_2^2 \rangle$ at small *n* but being felt mainly by $\langle L_1^2 \rangle$ at large *n*. Asymptotic limits at infinite *n* in Figure 10 yield $\langle L_2^2 \rangle / \langle L_1^2 \rangle = 0.19$, which is significantly smaller than the value of 0.326 obtained when all chain atoms contribute to the principal moments (Figure 7).[13,19] The actual numerical values for $\langle L_1^2 \rangle / nl^2$ and $\langle L_2^2 \rangle / nl^2$ at the asymptotic limits are, of course, larger in Figure 10 than in Figure 7. Charged chain ends are generally situated farther from their center of mass than the typical separation of a representative chain atom from the center of mass of all chain atoms.

Figure 11 depicts behavior of ratios of averages of corresponding principal moments for *f*-functional bolaforms having 20 bonds in each branch when chain ends provide the only atoms contributing to $\langle L_i^2 \rangle$. Asymmetries depicted in Figures 9 and 11 are strongly different at small *f*. Differences are most apparent with the linear bolaform, which has $\langle L_2^2 \rangle = \langle L_3^2 \rangle = 0$ when the only atoms considered are those at the chain ends. Differences in the asymmetries depicted in these two figures become smaller as *f* increases, particularly so when the stars are perturbed by repulsive interaction of the chains ends. Thus $\langle L_2^2 \rangle / \langle L_1^2 \rangle$ and $\langle L_3^2 \rangle / \langle L_1^2 \rangle$ are about 0.6 and 0.25, respectively, for the hexafunctional star in a medium with $D = 10$, irrespective of whether all chain atoms, or only those at the chain ends, contribute to the $\langle L_i^2 \rangle$. If branch point functionality is sufficiently high, asymmetry of the distribution described by the chain ends will be the same as the asymmetry of the distribution described by all chain atoms.

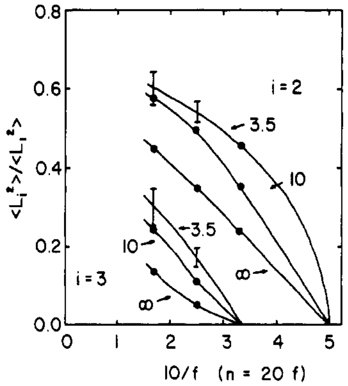

Figure 11. Ratios of averages of corresponding principal moments for the distribution of atoms at the chain ends in *f*-functional bolaforms having 20 bonds in each branch, the medium being assigned the indicated dielectric constant.

Conclusion. Configuration-dependent properties deduced for starlike polyethylenes bearing similarly charged ends are best summarized by considering macromolecules of three different sizes. No effects whatsoever are observed if *n* is so large as to be essentially infinite. The minimum *n* required to place a starlike polyethylene in this category depends on the configuration-dependent property under consideration. If that property is p_t, 10^3 bonds will qualify as infinite, but a much larger number of bonds is required if the property under consideration is $\langle s^2 \rangle$.

A second type of behavior is seen with small stars in which the number of bonds in each branch is on the order of 10. Here electrostatic interaction of the similarly charged chain ends produces a dramatic increase in the probability for a trans placement. Significant occupancy of gauche placements persists, however, because p_t does not reach unity. Stars of this size also experience an increase in their mean-square radii of gyration. Expansion occurs preferentially along the second principal axis, causing the stars to be driven toward (although they do not actually attain) a disklike distribution of chain atoms.

The third type of behavior is seen with *n* lying between those just described. In this region alterations in p_t are small or absent, but large increases in $\langle s^2 \rangle$ persist. The characteristic ratio passes through a maximum in this region if the medium is of sufficiently low dielectric constant. Expansion for starlike polyethylene now occurs preferentially along the major principal axis.

Perturbations produced by electrostatic interaction of charged chain ends would be smaller than those reported here if counterions or a supporting electrolyte were to be found in the vicinity of the stars.

Acknowledgment. This work was supported by National Science Foundation Research Grant PCM 78-22916. Acknowledgment is also made to the donors of the Petroleum Research Fund, administered by the American

Chemical Society, for partial support of this research.

References and Notes

(1) Rice, S. A.; Nagasawa, M. "Polyelectrolyte Solutions"; Academic Press: New York, 1961.
(2) Mattice, W. L.; Skolnick, J. *Macromolecules* **1981**, *14*, 863.
(3) Mattice, W. L.; Napper, D. H. *Macromolecules* **1981**, *14*, 1066.
(4) Smith, R. P. *J. Chem. Phys.* **1965**, *42*, 1162.
(5) Mattice, W. L.; Santiago, G. *Macromolecules* **1980**, *13*, 1560.
(6) Abe, A.; Jernigan, R. L.; Flory, P. J. *J. Am. Chem. Soc.* **1966**, *88*, 631.
(7) Patterson, G. D.; Flory, P. J. *J. Chem. Soc., Faraday Trans. 2* **1972**, *68*, 1098.
(8) Lide, D. R., Jr. *J. Chem. Phys.* **1960**, *33*, 1519.
(9) Mattice, W. L. *Macromolecules* **1975**, *8*, 644.
(10) Mattice, W. L.; Carpenter, D. K. *Macromolecules* **1976**, *9*, 53.
(11) Mattice, W. L. *J. Am. Chem. Soc.* **1976**, *98*, 3466.
(12) Jernigan, R. L.; Flory, P. J. *J. Chem. Phys.* **1969**, *50*, 4165.
(13) Mattice, W. L. *Macromolecules* **1980**, *13*, 506.
(14) Mansfield, M. L.; Stockmayer, W. H. *Macromolecules* **1980**, *13*, 1713.
(15) Mattice, W. L. *Macromolecules* **1981**, *14*, 143.
(16) Jernigan, R. L.; Flory, P. J. *J. Chem. Phys.* **1969**, *50*, 4178.
(17) Zimm, B. H.; Stockmayer, W. H. *J. Chem. Phys.* **1949**, *17*, 1301.
(18) Orofino, T. A. *Polymer* **1961**, *2*, 305.
(19) Solc, K. *Macromolecules* **1978**, *6*, 378.

Estimation of the χ Parameter for Poly(dimethylsiloxane) Solutions by the UNIFAC Group Contribution Method

Moshe Gottlieb* and Mordechay Herskowitz

Chemical Engineering Department, Ben Gurion University of the Negev, Beer Sheva, 84120 Israel.

Received April 14, 1981

ABSTRACT: The UNIFAC group contribution method is used to calculate the reduced residual chemical potential χ for poly(dimethylsiloxane) solutions in alkanes, aromatic hydrocarbons, and dimethylsiloxane oligomers. The correct dependence of χ on polymer segment fraction is obtained for all solvents. In most cases the computed value of χ differs by less than 10% from the experimental data. No adjustable parameters or solution data are required for the calculation. The UNIFAC method is shown to be a promising tool for systems with small "free volume" effects and unavailable experimental data.

The thermodynamics of polymer solutions have attracted the interest of many investigators. Several theories have been put forward in an effort to explain the various phenomena occurring when large polymer molcules are mixed with small solvent molecules.[1–5] Traditionally, the chemical potential (μ) or activity (a) of the solvent is described as the sum of two terms—a combinatorial term and a residual term:[2]

$$\ln a_1 = (\mu_1 - \mu_1^\circ)/RT = \{(\mu_1 - \mu_1^\circ)_{\text{comb}}/RT\} + \{(\mu_1 - \mu_1^\circ)_{\text{res}}/RT\} = \{\ln \phi_1 + (1 - 1/r)\phi_2\} + \chi\phi_2^2 \quad (1)$$

Here the subscripts 1 and 2 refer to the solvent and polymer, respectively, r is the ratio of molar volumes of polymer to solvent, and ϕ is the segment fraction defined as[3]

$$\phi_i = m_i v^*_{\text{sp},i}/(m_1 v^*_{\text{sp},1} + m_2 v^*_{\text{sp},2}) \quad (2)$$

where m_i is the mass of component i and $v^*_{\text{sp},i}$ is the core volume or characteristic volume per gram.

The combinatorial term in eq 1 is obtained from the Flory–Huggins lattice model. The residual term incorporates two distinct contributions: an "interactional" contribution due to differences in chemical nature between solvent and solute molecules and a "free volume" contribution due to volume changes involved in the mixing process.

The reduced residual chemical potential χ, defined by eq 1, is a key parameter in describing solution properties of non-cross-linked polymer molecules and swelling behavior of cross-linked materials.[6] Hence, the ability to predict its value over the entire range of polymer concentrations ($0 < \phi_2 < 1$) is the utmost test for the practical utility of any model. The lack of sufficient data on solution behavior for many important polymer–solvent pairs only emphasizes the need for a reliable predictive tool for the χ parameter.

Poly(dimethylsiloxane) (PDMS) is one of the most thoroughly studied polymers.[7] The relative abundance of data for various solvent–PDMS systems facilitates comparison of theory to experimental data. In addition, "free volume" effects are relatively small in PDMS solutions.[8] Such effects depend on the difference in free volume between the solution components. Most polymers exhibit considerably smaller free volume than those of typical solvents whereas PDMS, due to its high degree of thermal expansion, has a relatively large free volume. The negligible "free volume" contribution to χ enables one to study the "interactional" contribution independently. These two factors, combined with the practical importance of PDMS systems,[9] prompted us to concentrate in this work on PDMS solutions. Treatment of systems with large "free volume" effects will be considered in forthcoming publications.

Flory and Shih[10] have investigated the behavior of PDMS solutions in benzene, cyclohexane, and chlorobenzene. Utilizing their own data as well as data by Kuwahara et al.,[11] they have shown good agreement between experiment and Flory's theory.[2] The agreement is obtained with the aid of two adjustable parameters, X_{12} and Q_{12}, and manipulation of a third parameter s_1/s_2 between two limiting values. Chahal et al. in a recent publication[8] have compared 15 different PDMS–solvent systems to various one- and two-adjustable-parameter versions of Flory's theory. Their conclusions are that this theory fails to provide a reliable prediction of χ for each one of the tested solutions. Several other experimental studies on PDMS solutions are available,[7,22] but most of them are limited to

0024-9297/81/2214-1468$01.25/0